05,10

Features of the magnetic structure and properties of barium hexaferrite nanopowders obtained by hydrothermal synthesis

© A.Yu. Mironovich[1], V.G. Kostishyn[1], S.A. Melnikov[1], M.O. Kondratiev[1], E.S. Savchenko[1], A.G. Savchenko[1], A.I. Ril[2]

[1] „National University of Science and Technology „MISiS“, Moscow, Russia
[2] Lebedev Physical Institute, Russian Academy of Sciences, Moscow, Russia

E-mail: mironovich.ai@misis.ru

Received December 11, 2025
Revised December 11, 2025
Accepted December 24, 2025

This study investigated the influence of hydroxide ion (OH^-) concentration on the phase composition of barium hexaferrite ($BaFe_{12}O_{19}$) powders synthesized by the hydrothermal method. It was established that a significant excess of alkali in the reaction mixture ($OH/NO_3 > 16$ ratio) is necessary for the formation of a pure hexaferrite phase without impurities. Scanning electron microscopy demonstrated that the resulting powder consists of thin submicron platelets with well-defined facets. However, the internal structure of the particles is imperfect, which is evidenced by the X-ray diffraction patterns, Mössbauer spectra, and magnetic characteristics of the powder ($M_s = 18$ emu/g, $M_r = 3.7$ emu/g, $H_c = 0.35$ kOe). Annealing the particles leads to the elimination of defects and an improvement in the magnetic parameters ($M_s = 60$ emu/g, $M_r = 24$ emu/g, $H_c = 3.6$ kOe). It was demonstrated that uniaxial pressing of the obtained $BaFe_{12}O_{19}$ powder leads to the formation of a (00l)-type texture. After annealing at 900 °C, the pressed ferrite exhibits anisotropy of its magnetic properties, which is evidenced by a twofold difference in the squareness ratios of the magnetic hysteresis loops measured with the magnetic field applied parallel (0.3) and perpendicular (0.61) to the sample plane.

Keywords: Barium hexaferrite, Hydrothermal synthesis, Magnetic properties, Anisotropy, Crystallographic texture.

DOI: 10.61011/PSS.2026.01.63245.342-25

1. Introduction

Barium hexaferrite $BaFe_{12}O_{19}$ (BaM) is a well-known compound with a unique set of properties, especially magnetic ones: high coercive force, moderate saturation magnetization, high anisotropy constant, high ferromagnetic resonance frequency, and chemical stability. These properties determine the main practical applications of BaM: permanent magnets, microwave electronics devices, information storage devices.

In the last decade, the dependence of the functional characteristics of barium hexaferrite on its chemical composition ($BaFe_{12-x}Me_xO_{19}$, where Me — cations of various metals [1–5]), the method and conditions of synthesis and the forms of the resulting material (nano- and microdispersed powders [7], films [8], isotropic and anisotropic ceramics [9,10]) have been actively investigated [6]. The interest in hexaferrites is due to the need to solve urgent problems in the development of materials for 5G and 6G communication devices, more miniature or even planar microwave devices, permanent magnets that do not contain rare earths, as well as magnetic memory with high recording density. The material for such applications must first of all have anisotropy of magnetic properties. Anisotropic hexaferrites can be obtained using various principles and techniques, including epitaxial growth [11], particle orientation in a magnetic field [12], and self-texturing under uniaxial pressure [13].

The equilibrium grain shape of barium hexaferrite is a hexagonal plate. In this case, the crystallographic axis c, coinciding with the easy axis of magnetization, is directed along the normal to the plane of the plate. Hypothetically, such a structure makes it relatively easy to obtain anisotropic ceramic hexaferrite samples by sintering particles that are pre-oriented by applying pressure, a magnetic field, or their simultaneous action. In practice, the implementation of this approach is hampered by the peculiarities of the actual morphology of particles (deviation of shape from equilibrium, size, diameter to thickness ratio), as well as spontaneous aggregation (due to agglomeration and magnetic dipole-dipole interaction).

To obtain textured hexaferrites, it is preferable to use powders consisting of discrete crystallites with a large diameter-to-thickness ratio. At the moment, it is easiest to obtain barium hexaferrite in this state using the hydrothermal synthesis method. This technology makes it possible to synthesize various solid-phase substances from a solution [14–18], which allows crystallites to take a form close to equilibrium and independent of the morphology of

the particles of the initial reagents, as in the case of synthesis by solid-phase reactions.

To obtain barium hexaferrite, a mixture of a solution of iron and barium salts with a solution of a strong base is most often subjected to hydrothermal treatment. The essence of the technique seems to be quite simple, but a large number of possible synthesis parameters — temperature, time, type of reagents, their concentrations and ratios, autoclave volume — does not always allow for a quick selection of the optimal mode and get the desired result. In some cases, the target phase (hexaferrite) is practically impossible to obtain without subsequent high-temperature annealing [19,20].

At the moment, the following hypothesis of the formation of hexaferrite in hydrothermal conditions is widely accepted. First, mixing solutions of Fe^{3+} and OH^- produces ferrihydrite. It is believed that under hydrothermal conditions it dissolves to form complex ions $[Fe(OH)_4]^-$, which interact with each other and with barium ions to form the molecule $BaFe_{12}O_{19}$ [21]. The dissolution of ferrihydrite occurs when its active surface sites interact with ions/molecules of the solvent. The same sites are capable of adsorbing free metal cations [22,23]. In this regard, it was suggested in Ref. [24] that barium ions can be adsorbed on ferrihydrite and block solvent access to its active sites, which prevents the dissolution and further formation of barium hexaferrite. Analyzing the conditions of successful hydrothermal synthesis of BaM, it can be assumed that elevated temperatures or increased concentrations of hydroxide ions are required for the „unlocking" of surface sites. Indeed, many studies use a large excess of hydroxide anions (the ratio of $OH/NO_3 = 15.30$ [25–28]) [25–28]). On the other hand, some manage to obtain hexaferrite using smaller amounts of alkali ($OH/NO_3 = 2-5$ [29–31]). In this paper, the effect of the concentration of OH^- on the phase composition of powders obtained by hydrothermal treatment of a solution of Fe^{3+}, Ba^{2+} and OH^- is directly studied. It is demonstrated that an increase in the amount of free hydroxide anions in solution (under constant other synthesis conditions) actually leads to the formation of barium hexaferrite under hydrothermal conditions. In addition, it is shown that when the resulting BaM powders are pressed, a texture is formed in the compacts, leading to anisotropy of the magnetic properties.

2. Experimental part

The studied powders were obtained by hydrothermal synthesis. A mixture of an aqueous solution of ferric nitrate nonahydrate $Fe(NO_3)_3 \cdot 9H_2O$ and barium nitrate $Ba(NO_3)_2$ with an aqueous solution of sodium hydroxide NaOH in the ratio 40 ml/40 ml was used as a precursor. The solutions were prepared with the expectation that in the final volume (80 ml) the concentration of iron ions would be 0.1 mol/l, and the ratio Fe^{3+}/Ba^{2+} — 9 (as optimal for obtaining hexaferrite [32]). The amounts of NaOH were calculated in such a way that the OH/NO_3 ratio was 2.5, 5, 8, 12 and 16. In accordance with this ratio, the samples are labeled as BaM-2.5, BaM-5, etc. The resulting solutions were mixed in a 100 ml Teflon cup, which was loaded into an autoclave. The autoclave was placed in a muffle furnace, heated to 180 °C for 1 h and kept at this temperature for 4 h. The resulting precipitate was thoroughly washed with distilled water in a vacuum filtration unit, and then dried in a thermostat at 90 °C for 8 h, after which it was ground. For additional studies, a tablet with a diameter of 12 mm was made from the powder BaM-16 on a hydraulic press with a force of 4 t. The resulting tablet, as well as part of the powder, were annealed in air at 900 °C for 1 h (the heating rate was 15°/min, cooling was not controlled).

The phase analysis of the obtained samples was performed on Bruker D8 Advance X-ray diffractometers (radiation CuK_α, $\lambda = 0.154$ nm) and Bruker D2 PHASER. The obtained diffraction patterns were processed by the Rietveld method in the Profex program [33]. The magnetic parameters were measured using a vibration magnetometer JDAW-2000D. A Hitachi TM3030 scanning electron microscope was used to study the microstructure of the powder. The Mössbauer spectra of the samples were obtained using an EM MS-1104 setup with a Co^{57} source in a rhodium matrix.

3. Results and discussion

X-ray diffraction patterns of the obtained powders are shown in Figure 1. Based on the results of X-ray phase analysis, it can be concluded that the samples BaM-2.5 and BaM-5 consist of ferrihydrite, and BaM-12 and BaM-16 consist of barium hexaferrite. Reflexes of both phases are observed in the BaM-8 sample. This allows concluding that the OH/NO_3 ratio is one of the key parameters of the hydrothermal synthesis of BaM and a significant excess of alkali is required for the formation of the target phase. Also on the diffraction patterns of the samples BaM-2.5 and BaM-5 there is an amorphous halo on 31°. It may be due to the presence of a particularly fine fraction of ferrihydrite in the samples. According to the number of reflections on the diffraction pattern, the researchers distinguish two „types" of ferrihydrite — 2-linear and 6-linear. It is believed that the difference between these species is mainly due to the particle sizes [34]. Thus, it can be assumed that particles of various sizes are present in the samples, which leads to this type of diffraction patterns. At the same time, the center of the most intense peak (halo) of 2-linear ferrihydrite is expected to be found at 35°. However, doping with various elements can cause the center of the halo to shift, including by several degrees [35]. Since a large number of barium ions are present in the solution, it can be assumed that they enter the ferrihydrite structure. This can explain the shift of the halo of 2-linear ferrihydrite towards smaller angles, as well as the change in the ratio of reflex intensities of 6-linear ferrihydrite (compared with the literature data).

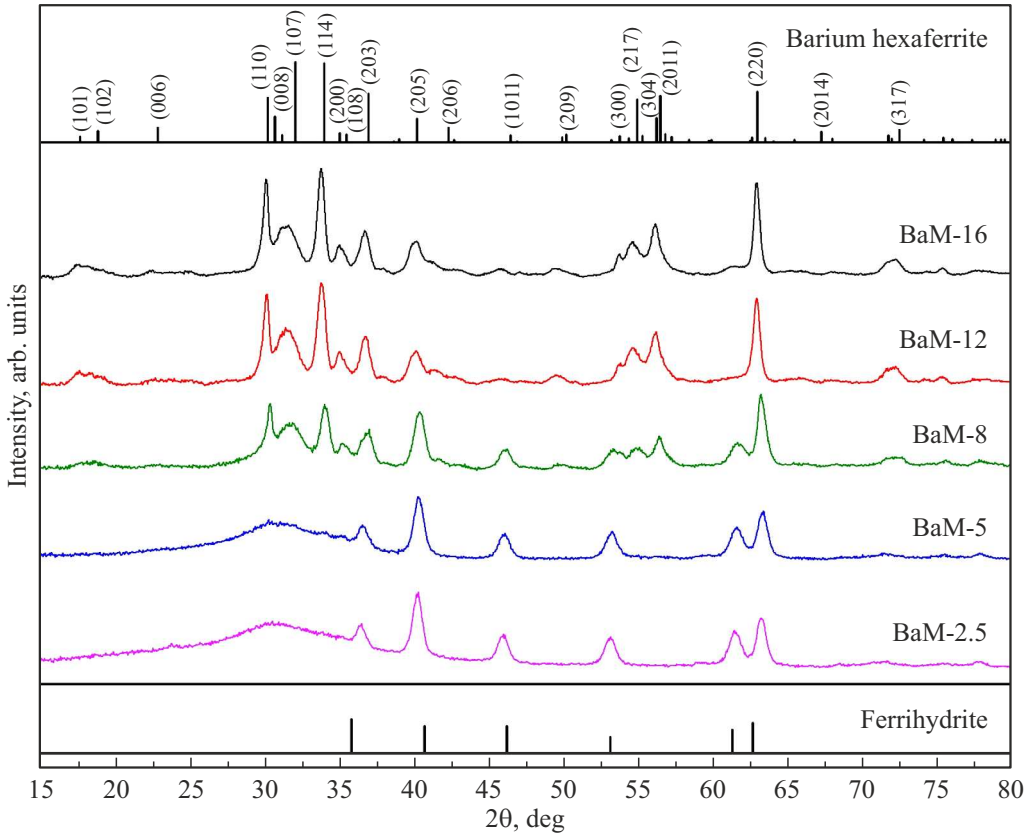

Figure 1. X-ray diffraction patterns of powders obtained with different OH/NO_3 ratios.

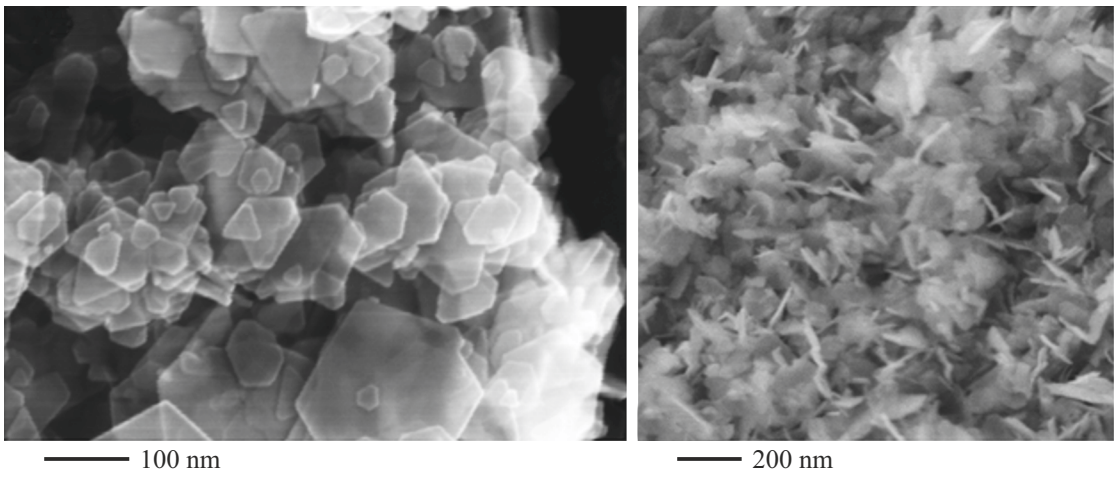

Figure 2. Electron micrographs of the sample BaM-16.

The widths of the different reflexes of hexaferrite are not the same, which indicates the anisotropic shape of the particles. This is especially noticeable in the range of angles 2θ from 30 to 35°: the reflex (110) is the narrowest, (107) is the widest, and (114) is intermediate. This configuration reflects the plate shape of the crystallites, in which the crystallographic axis c is directed normally to the plane of the plate, and the axes a and b lie in it. This is consistent with the electron micrographs of the BaM-16 sample shown in Figure 2. The resulting plate-like crystallites of hexaferrite have a thickness of no more than 20 nm and a width of 20 to 200 nm.

Despite the fact that the diffraction patterns of the samples BaM-12 and BaM-16 are almost identical, the actual phase composition of these powders may differ. It is known that the X-ray diffraction method has limitations

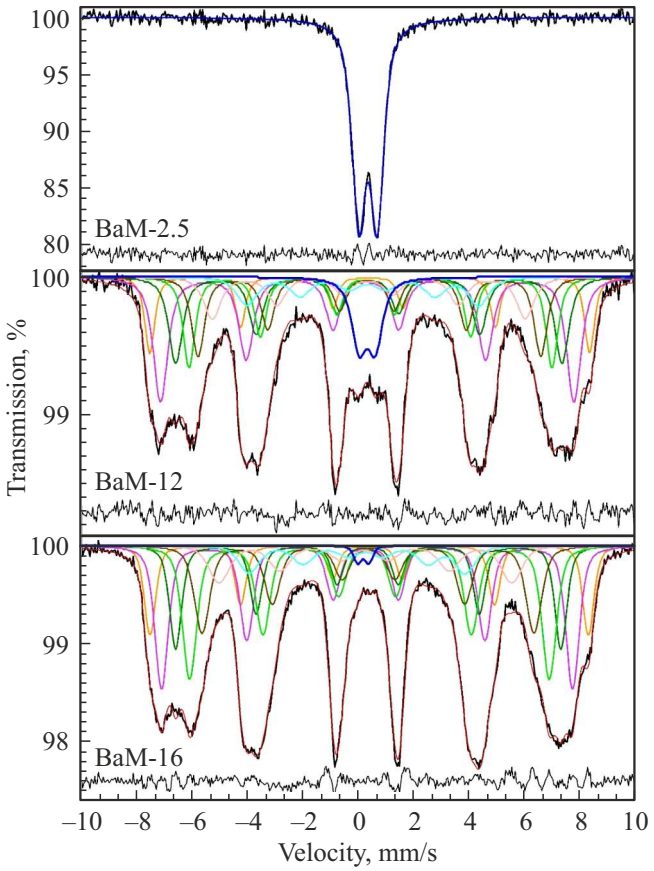

Figure 3. Mössbauer spectra of powders BaM-2.5, BaM-12 and BaM-16.

related to the size of the coherent scattering region and the degree of crystallinity of the samples. Thus, extremely small ferrihydrite particles with a weakly ordered structure may not appear on diffraction patterns. Therefore, to clarify the phase composition of the powders, Mössbauer spectroscopy was used, which has a higher resolution than the X-ray diffraction method.

The Mössbauer spectra of the samples are shown in Figure 3, and their parameters are listed in the table. The spectrum of the BaM-2.5 sample is a doublet with parameters corresponding to the ferrihydrite spectrum (isomer shift $IS = 0.35$ mm/s, quadrupole splitting $QS = 0.67$ mm/s) [36]. The spectra of BaM-12 and BaM-16 powders have an hyperfine magnetic structure, obviously caused by iron ions in the BaM lattice. The spectra were decomposed into 7 sextets, which is different from the number required for a spectrum of pure $BaFe_{12}O_{19}$ [37]. In addition, the parameters of the obtained sextets differ from those known in the literature [37]: the lower values of the magnetic fields on the ^{57}Fe nuclei are particularly noticeable. It should also be noted the relatively large width of the component lines. All these features can be attributed to two factors. Firstly, small particle sizes and, consequently, a large surface contribution. Secondly, the presence of a significant number of defects in the crystal lattice. Indeed, the dimensions of the coherent scattering region, calculated from the width of the X-ray reflections, are 23 and 7 nm in the directions [100] and [001], respectively. This is significantly smaller than the actual crystal sizes seen in Figure 2. Such a discrepancy is a sign of a high degree of defect in the crystal structure, which affects the appearance of X-ray diffraction patterns and Mössbauer spectra. Among the 7 sextets, it can be unambiguously determined by the isomer shift that the C2 component belongs to iron at position $4f_1$. Judging by the magnitudes of the magnetic fields (H_{eff}), sextets C1 and C3 correspond to iron at positions $2a/4f_2$. On the one hand, the sextet C3, as characterized by a smaller value of H_{eff}, should be attributed to the position $2a$, and C1 — to $4f_2$. On the other hand, in this case there is a discrepancy in relative areas: the theoretical value for $2a$ is 8.3 %, and for $4f_2$ — 16.7 %. This contradiction does not allow for a definitive determination of the correspondence of the sextets C1 and C3 to the positions $2a$ and $4f_2$. Sextets C4 and C5, according to their parameters, should be attributed to the non-equivalent positions of the $12k$ site. The C6 and C7 sextets are poorly resolved, and they are also characterized by non-standard parameter values for hexaferrite, which makes their interpretation difficult. Also, due to the strong overlap with

Parameters of the Mössbauer spectra of the obtained samples *

OH/NO_3	Component of spectrum	IS, mm/s	QS, mm/s	H_{eff}, kOe	S, %	Γ, mm/s
BaM-2.5	Ferrihydrite	0.35	0.67	–	100	0.58
BaM-12	C1 — $2a/4f_2$	0.35	0.07	492	12.1	0.49
	C2 — $4f_1$	0.28	0.07	462	20.3	0.56
	C3 — $2a/4f_2$	0.35	0.03	430	16.5	0.56
	C4 — $12k$	0.35	0.13	401	15.6	0.53
	C5 — $12k$-2	0.38	−0.04	373	15	0.7
	C6	0.22	−0.02	325	7	0.87
	C7	0.05	−0.38	231	6.7	0.87
	Ferrihydrite	0.33	0.66	–	6.8	0.67
BaM-16	C1 — $2a/4f_2$	0.36	0.06	490	11.4	0.48
	C2 — $4f_1$	0.29	0.05	460	21.9	0.58
	C3 — $2a/4f_2$	0.34	0.02	431	14.2	0.52
	C4 — $12k$	0.36	0.08	402	21.7	0.62
	C5 — $12k$-2	0.35	−0.02	371	15.3	0.66
	C6	0.24	0.03	327	8.5	0.87
	C7	0.1	−0.31	242	6.2	0.87
	Doublet	0.17	0.4	–	0.8	0.34

* IS, QS, H_{eff}, Γ and S accordingly, the isomer shift, quadrupole splitting, the effective magnetic field on the Fe^{57} nuclei, the line width, and the relative area of the component.

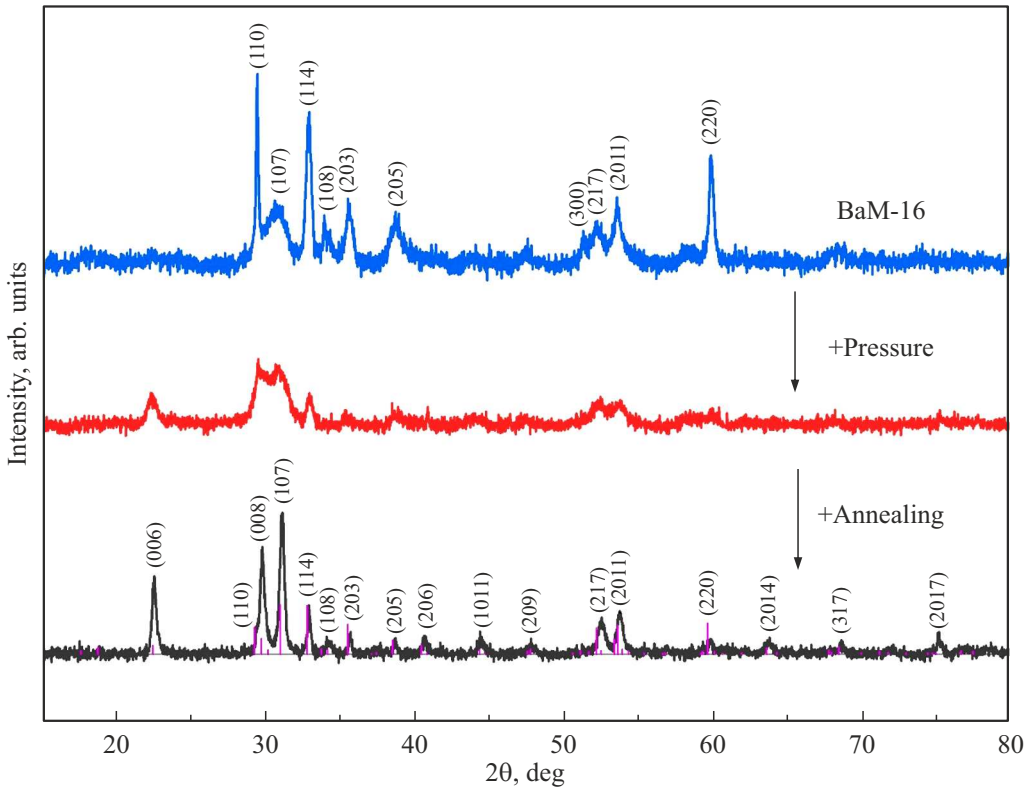

Figure 4. X-ray diffraction patterns of the BaM-16 sample after pressing and annealing.

other components in the spectrum, it was not possible to identify a sextet corresponding to position 2*b*.

In addition to sextets, a doublet is also present in the spectra of the samples BaM-12 and BaM-16. Doublet intensities — the main difference between these spectra. In the case of BaM-12, the doublet can be clearly distinguished, and it makes a significant contribution to the spectrum (6.8 %). On the contrary, the doublet area in the BaM-16 sample is negligible (< 1 %). The doublet parameters in the spectrum of BaM-12 correspond to those for BaM-2.5. Thus, it can be concluded that the BaM-12 sample contains a ferrihydrite fraction that is indistinguishable on X-ray diffraction patterns. In the case of BaM-16, the doublet parameters are different. On the one hand, this may be due to the inaccuracy of the fit due to the low intensity of the resonance lines. On the other hand, the appearance of such a doublet may be caused not by the presence of ferrihydrite, but by a contribution from the most defective regions near the surface of hexaferrite particles. Anyway, it follows from the results of Mössbauer spectroscopy that the sample BaM-16 contains a much higher amount of hexaferrite compared to BaM-12.

In connection with the obtained results, the sample BaM-16 was used for further experiments. Figure 4 shows diffraction patterns of the powder BaM-16 before pressing, as well as the tablet pressed from it before and after its annealing at 900 °C. It is possible to see that pressing leads to a significant transformation of the diffraction pattern. First of all, the appearance of the reflex (006) should be noted. Next, the intensity of reflexes (110) and (107) is equalized. The intensity of the remaining reflexes visibly decreases in relation to (107), and some of the reflexes disappear. All these changes indicate the ordering of particles and the formation of a texture (00l).

The annealing of ferrite, apparently, contributed to the elimination of defects and an increase in the coherent scattering region, which led to a narrowing of X-ray reflections. This made it possible to estimate the ratio of the intensities of different peaks and to characterize the texture of the sample more reliably.

The reflexes (114) and (107) are the most intense in the powder diffraction pattern of isotropic hexaferrite. In the case of peak (114), it can be said that its presence and intensity reflect the isotropy of the sample. Peak (107) cannot be estimated similarly, since in the case of a texture of type (00l) it may be caused by crystallites deflected by a small angle from the orientation axis. It is worth noting that such grains will still contribute to the anisotropy of the magnetic properties. Both peaks are present in the sample, but unlike isotropic powder, in which the intensity of these reflexes should be almost equal, in this case reflex (114) is almost 3 times weaker than reflex (107). To demonstrate inconsistencies, a stick diffraction pattern of isotropic barium hexaferrite powder, normalized by reflex (114), was superimposed on the diffraction pattern of the sample. It can be noted that the intensities of some

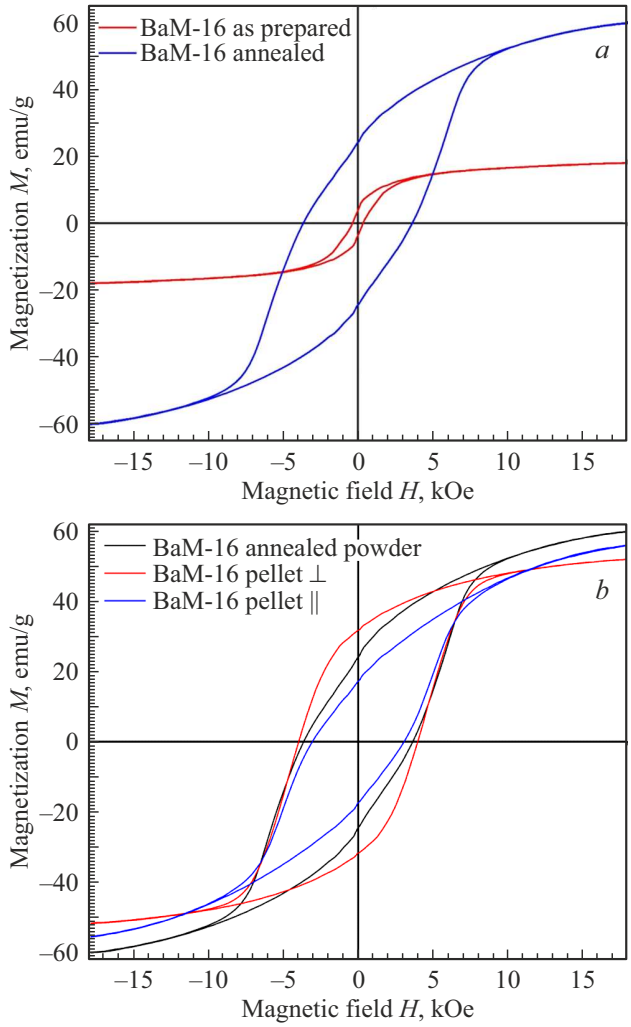

Figure 5. Magnetic hysteresis loops: *a* — powder BaM-16 before and after annealing; *b* — powder and tablet BaM-16 after annealing.

other peaks also differ from those expected for an isotropic sample. Thus, the ratios of reflex intensities (006) and (008) to intensity (107) for isotropic powder are on the order of 0.1 and 0.17, respectively. In the resulting sample, these values increase to 0.55 and 0.76, respectively. This allows considering the sample partially textured and expect anisotropy of its magnetic properties.

Figure 5, *a* shows the magnetic hysteresis loops of the powder BaM-16 before and after annealing at 900 °C. The magnetic parameters of the annealed powder are in good agreement with the known values for barium hexaferrite (saturation magnetization $M_s = 60$ emu/g, residual magnetization $M_r = 24$ emu/g, coercive force $H_c = 3.6$ kOe). Ferrite obtained directly from the autoclave, despite the fact that it exhibits magnetism, is significantly inferior in all parameters to the annealed sample.: $M_s = 18$ emu/g, $M_r = 3.7$ emu/g, $H_c = 0.35$ kOe. Apparently, such differences are due to the large number of defects in the crystal lattice of hydrothermally synthesized ferrite, as evidenced by the broadening of X-ray reflections and Mössbauer peaks, as well as the presence of additional components of the Mössbauer spectrum. Annealing eliminates defects, which leads to a significant increase in magnetic characteristics.

Figure 5, *b* shows the magnetic hysteresis loops of a tablet obtained from powder BaM-16 annealed at 900 °C. The measurements were carried out in a magnetic field applied perpendicular and parallel to the tablet plane. For comparison, Figure 5, *b* shows the hysteresis loop of the annealed powder. The differences in the presented hysteresis loops are evidence of the anisotropic nature of the magnetic properties of the sample. In particular, the powder loop, which can be considered isotropic in the first approximation, is characterized by a squareness ratio of 0.4. In the case of a tablet, this value depends on the position of the sample relative to the applied field and is 0.3 or 0.61 for parallel or perpendicular orientation, respectively. Similarly, the coercive force changes: for a powder, it is 3.6 kOe, and for a tablet, 3.96 or 3.06 kOe. The obtained results demonstrate that the BaM-16 tablet has an axis of easy magnetization directed along the normal to the sample plane, and an axis of hard magnetization parallel to the sample plane. These data are consistent with the above conclusions about the presence in the hexaferrite tablet of a texture induced by uniaxial pressing.

4. Conclusion

It has been experimentally confirmed that the OH/NO_3 ratio is a critical parameter of the hydrothermal synthesis of barium hexaferrite. A single-phase powder $BaFe_{12}O_{19}$ is formed only with a significant excess of alkali ($OH/NO_3 > 16$).

As a result of a comprehensive analysis using X-ray diffraction, Mössbauer spectroscopy, magnetometry, and electron microscopy, it was found that the sample obtained at $OH/NO_3 = 16$ consists of nanoplates of barium hexaferrite up to 20 nm thick and with a diameter of 20 to 200 nm with a high degree of defect in the crystal structure. Annealing at 900 °C eliminates defects and significantly improves the magnetic characteristics of the powder: saturation magnetization increases from 18 to 60 emu/g, residual magnetization from 3.7 to 24 emu/g, and coercive force from 0.35 to 3.6 kOe.

It was found that uniaxial pressing of the resulting barium hexaferrite powder leads to partial orientation of the plate-like particles and formation of a (00l) type texture in the compact. The sample obtained by uniaxial pressing of this powder followed by annealing demonstrates a pronounced anisotropy of magnetic properties. When measured in the direction perpendicular to the tablet plane, increased values of the coercive force (3.96 kOe) and the squareness ratio of the hysteresis loop (0.61) are observed compared with measurements in the parallel direction (3.06 kOe and 0.31) and with powder (3.6 kOe and 0.4).

Thus, the study demonstrates the effectiveness of the presented approach to the production of anisotropic ceramics $BaFe_{12}O_{19}$, which consists in the hydrothermal synthesis of discrete particles with plate-like morphology, their subsequent compaction by uniaxial pressing and annealing. The results obtained open up prospects for the creation of new materials based on barium hexaferrite for permanent magnets and microwave devices.

Funding

The study was supported by a grant provided by the Russian Science Foundation (Project No. 24-13-00268).

Conflict of interest

The authors declare that they have no conflict of interest.

References

[1] D.A. Vinnik, A.Yu. Starikov, V.E. Zhivulin, K.A. Astapovich, V.A. Turchenko, T.I. Zubar, S.V. Trukhanov, J. Kohout, T. Kmječ, O. Yakovenko, L. Matzui, A.S.B. Sombra, D. Zhou, R.B. Jotania, C. Singh, A.V. Trukhanov. Ceram. Int. **47**, *12*, 17293 (2021).
[2] K.P. Gafarova, V.E. Zhivulin, S.A. Gudkova, G.P. Vyatkin, L.A. Pesin, D.P. Sherstyuk, D.A. Vinnik. hSKh **65**, *9*, 132001 (2024) (in Russian).
[3] V.G. Kostishin, V.V. Korovushkin, K.V. Pokholok, A.V. Trukhanov, I.M. Isaev, A.Yu. Mironovich, M.A. Darvish. FTT **63**, *10*, 1496 (2021) (in Russian).
[4] V.V. Korovushkin, M.N. Shipko, V.G. Kostishin, I.M. Isayev, A.Yu. Mironovich, S.V. Trukhanov, A.V. Trukhanov. Neorgan. materialy **55**, *10*, 1065 (2019).
[5] D.P. Sherstyuk, A.I. Kovaleva, A.R. Zykova, V.E. Zhivulin, D.E. Zhivulin, D.A. Vinnik. ZhSKh **66**, *1*, 139712 (2025) (in Russian).
[6] D.V. Wagner, K.V. Kareva, V.A. Zhuravlev, O.A. Dotsenko, R.V. Minin. Inventions **8**, *1*, 26 (2023).
[7] P. Xu, X. Han, M. Wang. J. Phys. Chem. C **111**, *16*, 5866 (2007).
[8] V.G. Kostishin, A.Yu. Mironovich, A.V. Timofeev, R.I. Shakirzyanov, I.M. Isaev, G.A. Skorlupin, A.I. Ril. Mater. Today Commun. **31**, 103804 (2022).
[9] C.-C. Huang, C.-N. Wang, C.-C. Mo, H.-H. Hsu, IEEE Trans. Magn. **58**, *4*, 1 (2022).
[10] Y. Li, Q. Liu, M. Qi, Y. Chen. J. Electron. Mater. **52**, 523 (2023).
[11] V.G. Kostishin, A.Yu. Mironovich, A.V. Timofeev, I.M. Isaev, R.I. Shakirzyanov, G.A. Skorlupin, A.I. Ril. Superlattices Microstruct. **158**, 107005 (2021).
[12] F. Herrault, S. Cui, X.N. Guan, A.F. Gross. Microelectron. Eng. **236**, 111467 (2021).
[13] A.Z. Eikeland, F.H. Gjørup, H.L. Andersen, M. Christensen. RSC Adv. **14**, 10790 (2024).
[14] X. Jing, Y. Li, Q. Yin. Mater. Sci. Eng. B **99**, *1–3*, 506 (2003).
[15] I.J. Clark, T. Takeuchi, N. Ohtori, D.C. Sinclair. J. Mater. Chem. **9**, *1*, 83 (1999).
[16] Y. Zheng, E. Shi, S. Cui, W. Li, X. Hu. J. Am. Ceram. Soc. **83**, *10*, 2634 (2000).
[17] Y.A. Garanin, R.I. Shakirzyanov, D.I. Shlimas, M.A. Saidullayeva, D.B. Borgekov, M.E. Kaliyekperov. Crystals **15**, *10*, 904 (2025).
[18] Y. Garanin, R. Shakirziyanov, D. Borgekov, N. Volodina, D. Shlimas, M. Zdorovets. Sci. Rep. **15**, *1*, 26165 (2025).
[19] H. Vijayan, C.G. Knudsen, M.I. Mørch, M. Christensen. Mater. Chem. Front. **5**, *9*, 3699 (2021).
[20] E. Rezaie, A. Rezanezhad, L.S. Ghadimi, A. Hajalilou, N. Arsalani. Ceram. Int. **44**, *16*, 20285 (2018).
[21] M.L. Wang, Z.W. Shih, C.H. Lin. J. Cryst. Growth **114**, *3*, 435 (1991).
[22] M. Sajih, N.D. Bryan, F.R. Livens, D.J. Vaughan, M. Descostes, V. Phrommavanh, J. Nos, K. Morris. Geochim. Cosmochim. Acta **146**, 150 (2014).
[23] J.C. Mendez, T. Hiemstra. Geochim. Cosmochim. Acta **286**, 289 (2020).
[24] A.Y. Mironovich, V.G. Kostishin, G.A. Skorlupin, E.S. Savchenko, A.I. Ril. J. Cryst. Growth **656**, 128095 (2025).
[25] D. Primc, M. Drofenik, D. Makovec. Eur. J. Inorg. Chem. **2011**, *25*, 3802 (2011).
[26] S.E. Kushnir, A.I. Gavrilov, A.V. Grigorieva, D.D. Zaitsev, B.R. Churagulov, P.E. Kazin. ISJAEE, *11*(*115*), 45 (2012) (in Russian).
[27] D. Makovec, D. Primc, S. Šturm, A. Kodre, D. Hanžel, M. Drofenik. J. Solid State Chem. **196**, 63 (2012).
[28] M. Drofenik, I. Ban, G. Ferk, D. Makovec, A. Žnidaršič, A. Jagličić, D. Lisjak. J. Am. Ceram. Soc. **93**, *6*, 1602 (2010).
[29] Y. Li, A. Xia, C. Jin. J. Mater. Sci. Mater. Electron. **27**, *10*, 10864 (2016).
[30] A.Z. Eikeland, J. Hölscher, M. Christensen. J. Phys. D: Appl. Phys. **54**, *13*, 134004 (2021).
[31] A. Ataie, I.R. Harris, C.B. Ponton. J. Mater. Sci. **30**, *6*, 1429 (1995).
[32] A.Y. Mironovich, V.G. Kostishin, R.I. Shakirzyanov, A.A. Mukabenov, S.A. Melnikov, A.I. Ril, H.I. Al-Khafaji. J. Solid State Chem. **316**, 123625 (2022).
[33] N. Doebelin, R. Kleeberg. J. Appl. Crystallogr. **48**, *5*, 1573 (2015).
[34] F.M. Michel, L. Ehm, G. Liu, W.Q. Han, S.M. Antao, P.J. Chupas, P.L. Lee, K. Knorr, H. Eulert, J. Kim, C.P. Grey. Chem. Mater. **19**, *6*, 1489 (2007).
[35] G. Pieczara, M. Manecki, G. Rzepa, O. Borkiewicz, A. Gaweł. Mater. **13**, *18*, 4113 (2020).
[36] E. Murad. Clay Miner. **45**, *4*, 413 (2010).
[37] E.V. Pashkova, E.D. Solovyova, T.V. Kolodiazhnyi, V.P. Ivanitskii, A.G. Belous. J. Magn. Magn. Mater. **368**, 1 (2014).

Translated by A.Akhtyamov